ADVANCED FUNCTIONAL MATERIALS
www.afm-journal.de

Enhanced Performance of a ZnO Nanowire-Based Self-Powered Glucose Sensor by Piezotronic Effect

*Ruomeng Yu, Caofeng Pan, Jun Chen, Guang Zhu, and Zhong Lin Wang**

A self-powered, piezotronic effect-enhanced glucose sensor based on metal-semiconductor-metal (M–S–M) structured single ZnO nanowire device is demonstrated. A triboelectrical nanogenerator (TENG) is integrated to build a self-powered glucose monitoring system (GMS) to realize the continuously monitoring of glucose concentrations. The performance of the glucose sensor is generally enhanced by the piezotronic effect when applying a –0.79% compressive strain on the device, and magnitude of the output signal is increased by more than 200%; the sensing resolution and sensitivity of sensors are improved by more than 200% and 300%, respectively. A theoretical model using energy band diagram is proposed to explain the observed results. This work demonstrates a promising approach to raise the sensitivity, improve the sensing resolution, and generally enhance the performance of glucose sensors, also providing a possible way to build up a self-powered GMS.

1. Introduction

Glucose monitoring is one of the most important sensing technologies in medical science, clinical diagnostics, and food industry.[1] Glucose sensors, which accounts for 85% the market share of all the biosensor products,[2] attracted a huge amount of interest over the past decades.[3] In recent years, nanowires (NWs) based field effect transistors (FETs) were found to be a good candidate for bionsensing, which depends on the resistance change of the nanowires as chemical/biochemical species being adsorbed on the nanowire surface.[4] However, conventional NW-based glucose sensors still have some drawbacks, as it usually uses Ohmic contact in order to maximize the output signals, which works well provided the contact resistance is largely suppressed. Extremely small-size and small-diameter nanowires are desired in such sensors in order to enhance their sensitivity, which makes the fabrication more difficult and complex.

Recently, Schottky-contact based sensors have been demonstrated to exhibit much enhanced sensitivity and response time for gas, chemical and biochemical sensors, simply because the performance of the device is dictated by the local contact regardless the length or the size of the nanowires.[5–9] The Schottky-contact based sensor is much easier to fabricate using relatively large nanowires without sacrificing the desired sensitivity. Different from the Ohmic-contacted sensor, whose sensitivity is controlled by the "gate-voltage" like effect induced by the adsorbed species, a super-high sensitivity of the Schottky-contacted sensor is realized by using the local Schottky barrier height (SBH), which dominates the carrier transport process of the sensor and is very sensitive to the adsorption of surface charged/polar species. Using such a design, super-high sensitivity has been demonstrated for NW UV sensors,[10] biosensors,[6] and gas sensors.[7]

The optimum sensitivity of the sensor relies on an optimized SBH, because a too high SBH blocks the current to flow through, while a too low SBH is similar to an Ohmic-contacted device. As for wurtzite and zinc blend structured materials, the local SBH can be tuned by the piezotronic effect, which is about using strain-induced piezopotential as a "gate voltage" to tune/control the SBH across an interface or junction within a piezoelectric NW-based device.[10] It has been reported that piezotronic effect can greatly enhance the performance of piezoelectric NW-based Schottky-contact sensors such as strain sensor,[11] protein sensor,[8] pH sensor,[9] and photodetector[12] by tuning the effective SBH at the contacts.

Moreover, despite the dramatic decrease in size by employing NWs as build blocks of glucose sensors, it still requires power source to drive the sensors. Battery is the only way to power the device; however, no matter how compact the battery could be, it needs to be replaced after a certain period of time. It will be a huge benefit to have a self-powered glucose monitoring system (GMS) that can work sustainably without a battery.

In this work, we demonstrate a self-powered, piezotronic effect enhanced glucose sensor based on metal–semiconductor–metal (M–S–M) structured single ZnO nanowire device; a triboelectrical nanogenerator (TENG) was integrated to build a self-powered GMS to realize the continuously monitoring of glucose concentrations. The performance of the glucose sensor was generally enhanced by the piezotronic effect when applying a –0.79% compressive strain on the device, and the magnitude of the output signal was increased by more than 200%; the sensing resolution and sensitivity of sensors were improved by more than 200% and 300%, respectively. A theoretical model using energy-band diagram is proposed to explain the observed

R. M. Yu, Dr. C. F. Pan, J. Chen, G. Zhu, Prof. Z. L. Wang
School of Materials Science and Engineering
Georgia Institute of Technology
Atlanta, GA 30332-0245, USA
E-mail: zhong.wang@mse.gatech.edu
Dr. C. F. Pan, Prof. Z. L. Wang
Beijing Institute of Nanoenergy and Nanosystems
Chinese Academy of Sciences, Beijing, China

DOI: 10.1002/adfm.201300593

results. This work demonstrates a promising approach to raise the sensitivity, improve the sensing resolution and generally enhance the performance of glucose sensors, also providing a possible way to build up a self-powered GMS.

2. Results and Discussion

By surface functionalizing with glucose oxidase (GOx), a ZnO NW-based glucose sensor with Schottky contact is fabricated. ZnO nanostructures, due to their biocompatibility, stability, and high isoelectric point,[13–14] have been widely reported in application of glucose sensing.[14–16] Furthermore, as a member of the wurzite structure family, ZnO has piezoelectric properties, making it a good candidate for studying the piezotronic effect on the glucose sensor. ZnO NWs used in this work were synthesized via a high temperature thermal evaporation process,[11,17] with length of several hundreds of micrometers and diameter varying from tens of nanometers to a few micrometers. The glucose sensor was fabricated by transferring and bonding an individual ZnO NW laterally onto a polyethylene terephthalate (PET)/or a polystyrene (PS) substrate, with its *c*-axis in the plane of the substrate pointing to the source. Silver paste was used to fix the two ends of the NW, serving as the source and drain electrodes, respectively. A thin layer of epoxy was applied to isolate both end-electrodes from the environment in order to avoid potential contacting between electrodes and the glucose solution during the measurements. For the surface decoration, 0.005 mL GOx with a concentration of 10 mg mL^{-1} was added onto the NW and incubated for two hours in the fume hood to dry naturally;[16] this process was repeated four times followed by rinsing with deionized (DI) water to remove those non-firmly adsorbed GOx; then, the devices were ready to perform as glucose sensors. A schematic in **Figure 1** a shows a GOx-decorated strain free ZnO NW glucose sensor in glucose solution. The same device under compressive strain is presented in Figure 1b. A real device is given in Figure 1d (inset).

The response of the ZnO NW glucose sensors to different strains was investigated by applying a compressive strain step by step, up to –0.79%, with the sensors totally immersed in pure DI water instead of glucose solution. Experiment set-up is shown in the inset of Figure 1e, one end of the device was fixed tightly on a manipulation holder, while the other end was free to be bent by a three-dimensional mechanical stage with movement step resolution of 1 μm. The magnitude of compressive strains can be calculated according to Yang et al.'s work.[18] Figure 1d presents the *I*–*V* characteristics of a device when applied different compressive strains. It is obvious to see that the output signal (i.e., currents) experienced a tremendous increase as the device was compressively bent. At a bias voltage of 1.8 V, the current increased from 0.15 μA all the way to more than 25 μA, which is about 150 times larger in magnitude, as a –0.79% compressive strain was applied. Since ZnO is a piezoelectric semiconductor, an externally applied strain would produce piezo-charges at the interfacial region. It is important to note that these are ionic and non-mobile charges adjacent to the interface and thus cannot be completely screened. The positive piezo-charges may effectively lower the barrier height at the local Schottky contact (Φ_d), while the negative piezo-charges increase the barrier height (Φ_s). Such tuning of the effective SBH would then largely change the transport process of the ZnO NW sensors, which is known as piezotronic effect. This is the mechanism of the observed ZnO NW sensors response to strains. Although piezoresistance effect should also contribute to the variation of the resistance of ZnO sensors under externally applied strain, it cannot be the dominant factor. Instead of tuning the M–S contact characteristics like piezotronic effect, piezoresistance effect is realized by changing the inter-atomic spacing and thus affecting the bandgap of ZnO. The change of the resistance can be calculated via[19]

$$\frac{\Delta R}{R} = \pi_l \Delta\sigma_l + \pi_t \Delta\sigma_t \quad (1)$$

where R is the resistance, ΔR is the change of resistance, π_l and π_t are the longitudinal and transverse piezoresistive effect coefficient, and $\Delta\sigma_l$ and $\Delta\sigma_t$ are the changes in stress applied to the longitudinal and transverse direction of ZnO NWs. In this work, at a bias voltage of 1.8 V, the resistance difference between unstrained and –0.79% compressively strained sensor, $\Delta R/R$, is around 166. $\Delta\sigma_l$ is 104 GPa, $\Delta\sigma_t$ can be ignored compared with $\Delta\sigma_l$. If piezoresistive effect dominated the change of ZnO NW sensor, a calculation followed the Equation 1 will give the value of $\pi_l = 16\,000 \times 10^{-11}$ Pa^{-1}, which is almost 4 orders of magnitude higher than a typical value in the 10^{-11} level. This result indicates that it is the piezotronic effect, rather than the piezoresistive effect, which has played an essential role in tuning the output signals of ZnO NW glucose sensors.

The response of a strain free ZnO glucose sensor to different glucose concentrations is presented in Figure 1e, measured at a fixed bias of 2 V. By gradually adding glucose into the solution drop by drop, the output signal clearly increased step by step as expected. At each step, the current stayed at a distinguishable value for more than 10 s, which shows a good response and stability of the ZnO NW glucose sensors. The detection limit of the ZnO NW glucose sensors can be as low as 0.49 mg L^{-1} (2.7 μM), the experimental results are presented in the Supporting Information, Figure S4. Being able to respond to the glucose concentrations ranging from 0.09 g L^{-1} to 1.5 g L^{-1}, the ZnO NW glucose sensor can cover the typical range of human body blood sugar level which is 0.8 g L^{-1} to 1.2 g L^{-1}, making it a qualified candidate for GMS.

A TENG, reported by our group previously,[20] was integrated as the power source to drive the ZnO NW glucose sensor for building a self-powered GMS. Figure 1f shows the voltage across the glucose sensor versus different glucose concentrations ranging from 0 g L^{-1} to 2.14 g L^{-1}. The good stability of this self-powered GMS was well indicated by the output voltage across the glucose sensor under each glucose concentration, as presented in Figure 1f. Besides, it can be seen that, as the glucose concentrations increased, the component voltage across ZnO glucose sensor decreased step by step. This behavior was controlled by the same mechanism as that of glucose sensor output signals response to glucose concentrations. Since the product of reaction between glucose and GOx, H_2O_2, can transfer electrons onto the ZnO NW surface, and thus increase the charge carrier density, the higher the glucose concentration, the higher the carrier density, and the lower the resistance of the glucose sensor. Therefore, the component voltage across

Adv. Funct. Mater. **2013**,
DOI: 10.1002/adfm.201300593

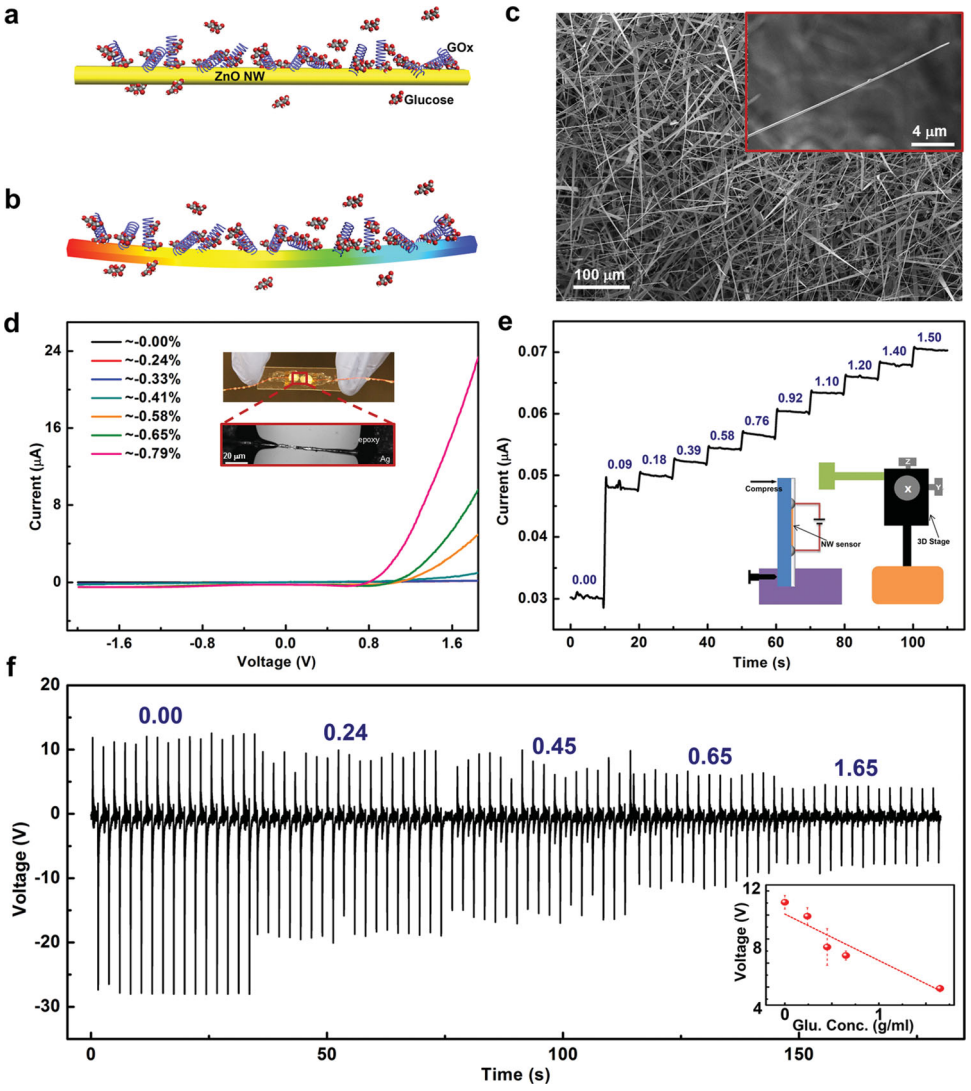

Figure 1. Schematic of ZnO NW decorated with GOx surrounded by glucose molecules under a) no strain and b) compressive strain. c) SEM image of the morphology of the as-synthesized ZnO NWs. The inset presents a single ZnO NW in higher resolution. d) *I–V* characteristics of a ZnO NW glucose sensor under different compressive strains, no glucose added. The inset shows a digital image and an optical microscopy image of the ZnO NW glucose sensor. e) *I–t* characteristics of another ZnO NW glucose sensor in different glucose concentrations, no external strains applied. The inset presents a schematic of the experiments set-up. f) *V–t* characteristics of the ZnO NW glucose sensor as for d) in different glucose concentrations, when integrated with a TENG, numbers labeled in unit of (g L^{-1}). The inset is a plot of voltage across the sensor (*V*) vs. glucose concentrations (g L^{-1}). Data were extracted from the "upper-side" of the *V–t* curve in (f). A linear fit of the experimental data is presented as red straight line.

the glucose sensor dropped down when increasing the glucose concentrations, as presented in Figure 1f.

I–t and *I–V* characteristics of the devices at different strains and various glucose concentrations were recorded to investigate the piezotronic effect on the performances of ZnO NW-based glucose sensors. Two series of experiments were carried out by changing the strains and glucose concentrations simultaneously: the first series of experiments were conducted by adding glucose solution step by step under a fixed compressive strain at each time; the *I–t* characteristics of a glucose sensor under compressive strain –0.33% and –0.79% are presented in **Figure 2**a,b, respectively. More *I–t* characteristics of a glucose sensor under compressive strain of –0.50%, –0.58%, –0.65%, and –0.71% are shown in Supporting Information, Figure S1a–d, respectively. It can be seen that the overall output signals were increased by a large amount when increased the compressive strain. Moreover, it is easier to tell the current difference between two glucose concentrations when increasing the externally applied strain. For example, under –0.33% strain (Figure 2a), the current response to 0.18 g L^{-1} and 0.39 g L^{-1} glucose concentrations hardly differed from each other, while that difference between the same glucose concentrations under –0.79% compressive strain (Figure 2b) became much more obvious. This result indicates that the piezotronic effect can improve the sensing resolution of the glucose sensor, which is due to the non-linear *I–V* transport properties created by the Schottky barrier at the contacts of the M–S–M structure, similar to an amplification effect. By resolution, here, we mean the

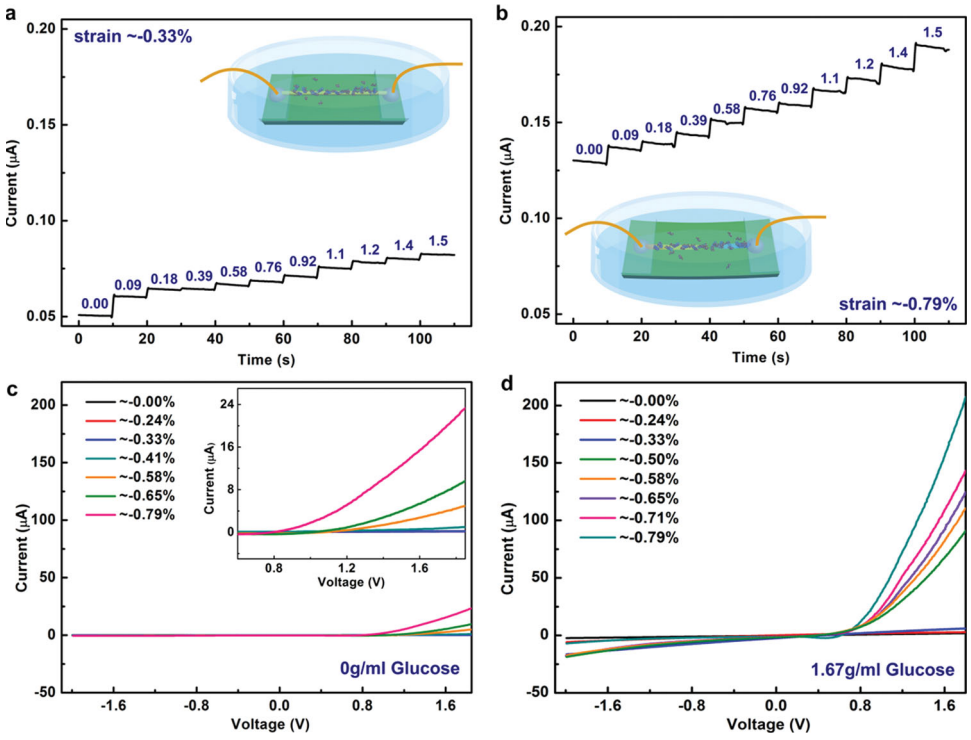

Figure 2. *I–t* characteristics of a ZnO NW glucose sensor in different glucose concentrations, numbers labeled in unit of (g L^{-1}), under a) –0.33% compressive strain and b) –0.79% compressive strain. The insets are schematics of adding glucose step by step to the glucose sensor under –0.33% and –0.79% compressive strain, respectively. *I–V* characteristics of the ZnO NW glucose sensor under different compressive strains, in a certain glucose concentration of c) 0 g L^{-1} and d) 1.67 g L^{-1}. The inset of (c) is an enlarged *I–V* curve to present more details.

ability of the smallest concentration change that can be distinguished by the sensor and the measuring system. The second series experiments were conducted by applying compressive strains step by step in glucose solution of a certain concentration at each time; the *I–V* characteristics of a device in glucose solution of concentration 0 g L^{-1} and 1.67 g L^{-1} are shown in Figure 2c,d, respectively. It is obvious that the current went up by tens of times in magnitude when the glucose concentration was increased. This result again confirms the former conclusion that the higher the glucose concentration, the higher the output signals. The results in Figure 2 indicate that ZnO NW glucose sensors have good response to both strains and glucose concentrations at the same time; the output signal increases as either increasing the compressive strain or the glucose concentration. Furthermore, the piezotronic effect can also improve the sensing resolution of the ZnO NW glucose sensors.

By systematically investigating the glucose sensors response to continuously changed compressive strains and glucose concentrations, a three-dimensional surface graph was plotted, as presented in **Figure 3**a. An overall trend of how the output signal varied with changing both the compressive strains and glucose concentrations can be simultaneously derived from this 3D graph. The current clearly went up as the glucose concentration or the compressive strain increased. Four 2D graphs are shown in Figure 3b–e for more details and information, which are extracted from Figure 3a by projecting on *I*–strain surface and *I*–glucose concentration surface, respectively. Figure 3b,c show the absolute and relative current response of ZnO NW glucose sensors to various glucose concentrations when the compressive strain was fixed in each curve, ranging from –0.00% to –0.79%, respectively. Figures 3d,e present the absolute and relative current response of ZnO NW glucose sensors to different compressive strains under a certain glucose concentration in each curve, differing from 0.00 g L^{-1} to 1.50 g L^{-1}, step by step. The results in Figure 3b show that increasing the compressive strain can lead to an enlarged output signal, which again confirms that the piezotronic effect can generally enhance the performance of ZnO NW glucose sensors by rising up the signal level. Moreover, the slope of curves became deeper and deeper when the applied strain increased, which means the sensing resolution is improved by the piezotronic effect. The same improvement can be derived more easily from Figure 3d, which indicates that the current difference between two certain glucose concentrations was significantly enlarged when applying more compressive strain. For example, under 0% strain, the current difference between 0.09 g L^{-1} and 1.5 g L^{-1} glucose concentration was 0.023 μA, while the same difference under –0.79% strain was enlarged to 0.053 μA, more than 200% increase in magnitude was observed in this case. This observation again confirmed another influence of the piezotronic effect on the ZnO glucose sensor performance: improving the sensing resolution of sensors. From Figure 3c it can be seen that the relative change in current by adding glucose can be as large as 130% and mostly around 25% to 50%. In Figure 3e, this relative change in current has the largest value above 300% and mostly around 150%, when applied

Adv. Funct. Mater. **2013**,
DOI: 10.1002/adfm.201300593

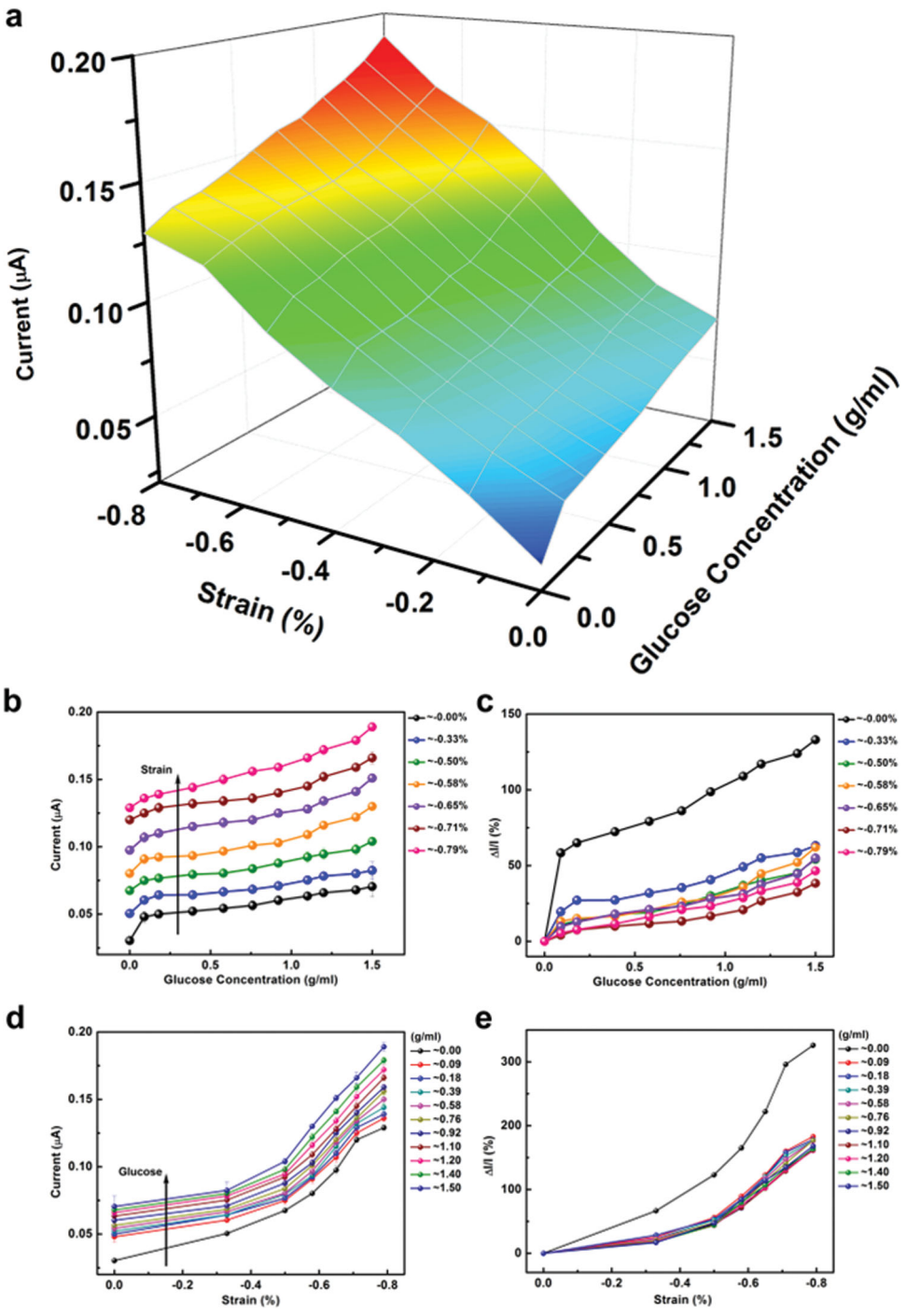

Figure 3. Piezotronic effect on the performances of ZnO NW glucose sensors. a) 3D surface graph indicating the current response of the ZnO NW glucose sensor under different strains and glucose concentrations. b,c) Absolute and relative current response of the ZnO NW glucose sensor in different glucose concentrations, with compressive strain ranging from 0 to –0.79%, respectively. d,e) Absolute and relative current response of the ZnO NW glucose sensor under different compressive strains, with glucose concentration ranging from 0 to 1.50 g L^{-1}, respectively. Data of (b–e) were extracted from (a).

more compressive strains. These results indicate that applying strains can significantly improve the sensitivity of glucose sensors; the relative change of output signals in this case is even much larger than in the case of adding glucose. Therefore, the piezotronic effect can largely improve the sensitivity of ZnO NW glucose sensors.

A theoretical model is proposed to explain the piezotronic effect on the performances of ZnO NW glucose sensors using

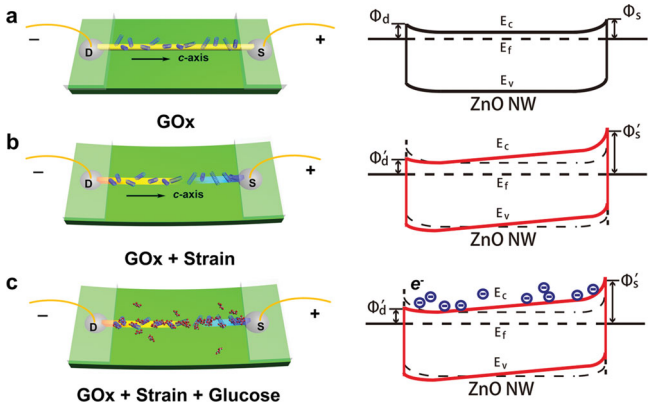

Figure 4. Schematic energy band diagrams of ZnO NW glucose sensors explaining their performances when they are a) unstrained (presented as black solid lines in (a), black dashed lines in (b) and (c), b) compressively strained and functionalized with GOx, surrounded by no glucose molecules (presented as red solid lines in (b), red dashed lines in (c), c) compressively strained and functionalized with GOx, surrounded by glucose molecules (presented as red solid lines in (c)).

energy band diagrams, as presented in **Figure 4**. The energy band structure of a strain free ZnO NW glucose sensor is presented in Figure 4a. In an M–S–M structure with *c*-axis pointing from drain to source, as shown in Figure 4a, the transport process of the ZnO NW glucose sensor would be dominated by the reversely biased Schottky barrier, that is, Φ_d here with very high sensitivity. Figure 4b shows the energy band structure of a glucose sensor subject to compressive strains. When applying a compressive strain, piezo-charges occurred at the M–S contact with the *c*-axis pointing at the negative-charge side. It is important to note that the polarized charges are ionic charges, which are non-mobile charges located around the M–S interfacial region. Under this circumstance, free carriers can only partially screen the piezo-charges but they cannot completely cancel out all of them. The positive piezo-charges may effectively lower the height of Φ_d at the local contact, while the negative piezo-charges increase the height of Φ_s, as presented in Figure 4b. As a result, the local SBH Φ_d, which was in dominance of the transport process,[21] became lower when increased the externally applied compressive strain, and thus led to a higher output signal of the ZnO NW glucose sensors. It is by this way that the externally applied compressive strains changed the local contact characteristics through an internal field at the M–S interfacial region and played an essential role in tuning the carrier transport process.[22]

The working principle of a compressively strained ZnO NW glucose sensor under a certain glucose concentration is illustrated by an energy-band structure shown in Figure 4c. When glucose reacts with GOx, gluconic acid and H_2O_2 are produced according to the following formula:

$$\text{D-glucose} + H_2O + O_2 \xrightarrow{\text{GOx}} \text{D-gluconic acid} + H_2O_2 \quad (2)$$

It has been reported that H_2O_2 can transfer electrons onto the surface of ZnO NW,[15] which is equivalent to increase the carrier density within n-type ZnO NW based glucose sensor, as shown in Figure 4c. Therefore, the more glucose in solution, the higher the carrier density in n-type glucose sensor, and the higher the output signal of the glucose sensors. This explains why the output signal increased as adding more glucose into the solution.

3. Conclusions

An M–S–M structured ZnO NW glucose sensor was presented to work as a glucose sensor. A TENG was integrated with ZnO glucose sensor to work as a self-powered GMS. The piezotronic effect on the performance of the ZnO glucose sensor was systematically studied by varying both the compressive strains and glucose concentrations. The results indicate that piezotronic effect can significantly raise the sensitivity as well as improve the sensing resolution of ZnO NW glucose sensors. A theoretical model using energy band structure is proposed to explain the observed results. This work introduces a promising approach to raise the sensitivity, improve the sensing resolution, and generally enhance the performance of glucose sensors, also providing a possible way to build up a self-powered GMS.

Supporting Information

Supporting Information is available from the Wiley Online Library or from the author.

Acknowledgements

R.M.Y and C.F.P. contributed equally to this work. This research was supported by NSF, BES DOE (DE-FG02-07ER46394), and the Knowledge Innovation Program of the Chinese Academy of Science (Grant No. KJCX2-YW-M13).

Received: February 15, 2013
Revised: March 29, 2013
Published online:

[1] J. Wang, *Chem. Rev.* **2008**, *108*, 814.
[2] A. Heller, B. Feldman, *Chem. Rev.* **2008**, *108*, 2482.
[3] a) J. Shah, E. Wilkins, *Electroanal.* **2003**, *15*, 157; b) J. M. Zen, C. W. Lo, *Anal. Chem.* **1996**, *68*, 2635.
[4] a) M. Ahmad, C. F. Pan, Z. X. Luo, J. Zhu, *J. Phys. Chem. C* **2010**, *114*, 9308; b) F. Patolsky, G. F. Zheng, C. M. Lieber, *Anal. Chem.* **2006**, *78*, 4260.
[5] J. Zhou, Y. D. Gu, Y. F. Hu, W. J. Mai, P. H. Yeh, G. Bao, A. K. Sood, D. L. Polla, Z. L. Wang, *Appl. Phys. Lett.* **2009**, *94*, 191103.
[6] P. H. Yeh, Z. Li, Z. L. Wang, *Adv. Mater.* **2009**, *21*, 4975.
[7] T. Y. Wei, P. H. Yeh, S. Y. Lu, Z. Lin-Wang, *J. Am. Chem. Soc.* **2009**, *131*, 17690.
[8] R. M. Yu, C. F. Pan, Z. L. Wang, *Energ. Environ. Sci.* **2013**, *6*, 494.
[9] C. F. Pan, R. M. Yu, S. M. Niu, G. Zhu, Z. L. Wang, *ACS Nano* **2013**, DOI: 10.1021/nn306007p.
[10] Z. L. Wang, *Adv. Mater.* **2012**, *24*, 4632.
[11] J. Zhou, Y. D. Gu, P. Fei, W. J. Mai, Y. F. Gao, R. S. Yang, G. Bao, Z. L. Wang, *Nano Lett.* **2008**, *8*, 3035.
[12] Q. Yang, X. Guo, W. H. Wang, Y. Zhang, S. Xu, D. H. Lien, Z. L. Wang, *ACS Nano* **2010**, *4*, 6285.

[13] a) C. Yang, C. X. Xu, X. M. Wang, *Langmuir* **2012**, *28*, 4580; b) C. Satriano, M. E. Fragala, Y. Aleeva, *J. Colloid Interface Sci.* **2012**, *365*, 90.
[14] Y. L. Zhai, S. Y. Zhai, G. F. Chen, K. Zhang, Q. L. Yue, L. Wang, J. F. Liu, J. B. Jia, *J. Electroanal. Chem.* **2011**, *656*, 198.
[15] a) K. Singh, A. Umar, A. Kumar, G. R. Chaudhary, S. Singh, S. K. Mehta, *Sci. Adv. Mater.* **2012**, *4*, 994; b) S. Palanisamy, A. T. E. Vilian, S. M. Chen, *Int. J. Electrochem. Sci.* **2012**, *7*, 2153; c) S. Park, K. Cho, S. Kim, *Microelectron. Eng.* **2011**, *88*, 2611; d) S. M. U. Ali, Z. H. Ibupoto, S. Salman, O. Nur, M. Willander, B. Danielsson, *Sens. Actuators, B* **2011**, *160*, 637; e) S. M. U. Ali, T. Aijazi, K. Axelsson, O. Nur, M. Willander, *Sensors* **2011**, *11*, 8485; f) X. W. Liu, Q. Y. Hu, Q. Wu, W. Zhang, Z. Fang, Q. B. Xie, *Colloid Surf., B* **2009**, *74*, 154; g) H. B. Liu, X. M. Qian, S. Wang, Y. L. Li, Y. L. Song, D. B. Zhu, *Nanoscale Res. Lett.* **2009**, *4*, 1141; h) J. F. Zang, C. M. Li, X. Q. Cui, J. X. Wang, X. W. Sun, H. Dong, C. Q. Sun, *Electroanal.* **2007**, *19*, 1008.
[16] Y. M. Sung, K. Noh, W. C. Kwak, T. G. Kim, *Sens. Actuators, B* **2012**, *161*, 453.
[17] a) Z. W. Pan, Z. R. Dai, Z. L. Wang, *Science* **2001**, *291*, 1947; b) M. Eichenfield, J. Chan, R. M. Camacho, K. J. Vahala, O. Painter, *Nature* **2009**, *462*, 78.
[18] R. S. Yang, Y. Qin, L. M. Dai, Z. L. Wang, *Nat. Nanotechnol.* **2009**, *4*, 34.
[19] S. M. Sze, *Semiconductor Sensors*, Wiley Interscience, New York **1994**.
[20] a) G. Zhu, C. F. Pan, W. X. Guo, C. Y. Chen, Y. S. Zhou, R. M. Yu, Z. L. Wang, *Nano Lett.* **2012**, *12*, 4960; b) Z. L. Wang, G. Zhu, Y. Yang, S. H. Wang, C. F. Pan, *Mater. Today* **2012**, *15*, 532.
[21] R. M. Yu, L. Dong, C. F. Pan, S. M. Niu, H. F. Liu, W. Liu, S. Chua, D. Z. Chi, Z. L. Wang, *Adv. Mater.* **2012**, *24*, 3532.
[22] Z. L. Wang, *Nano Today* **2010**, *5*, 540.